Research Article Vol. 32, No. 5 / 26 Feb 2024 / Optics Express 8081
Optics EXPRESS

Adaptive-memory-length look-up table (LUT)-based digital pre-distortion for IM/DD underwater wireless optical communications

YANTING ZHOU,[1,2,†] JUNWEI ZHANG,[3,4,†] CHAO LU,[3,4] ZABIH GHASSEMLOOY,[5] AND CHANGJIAN GUO[1,2,*]

[1]*Guangdong Key Laboratory of Optical Information Materials and Technology, South China Academy of Advanced Optoelectronics, South China Normal University, Guangzhou, China*
[2]*National Center for International Research on Green Optoelectronics, South China Normal University, Guangzhou 510006, China*
[3]*Photonics Research Institute, Department of Electronic and Information Engineering, The Hong Kong Polytechnic University, Hong Kong (SAR), China*
[4]*School of Electronics and Information Technology, Sun Yat-sen University, Guangzhou 510275, China*
[5]*Optical Communications Research Group, Faculty of Engineering and Environment, Northumbria University, Newcastle Upon Tyne NE1 8ST, United Kingdom*
[†]These authors contributed equally to this work.
[*]*changjian.guo@coer-scnu.org*

Abstract: A digital pre-distortion (DPD) scheme based on an adaptive-memory-length look-up table (AML-LUT) is proposed and experimentally demonstrated in a four-level pulse amplitude modulation (4-PAM) underwater optical wireless communication (UOWC) system. By implementing adaptive memory length for each pattern in the AML-LUT-based DPD, the size of the AML-LUT can be significantly reduced without sacrificing performance compared to both the full-size LUT and the multi-symbol simplified look-up table (MSS-LUT)-based DPDs. The performance of the proposed AML-LUT-based DPD is experimentally evaluated for a 625 Mbit/s 4-PAM UOWC over 1 m transmission length. Experimental results show that compared with the full-size LUT with a memory length of 7 (LUT-7)-based DPD, the proposed AML-LUT-based DPD (i) incurs a marginal power penalty of 0.5 dB at both the 7% hard-decision forward error correction (HD-FEC) and KP4-FEC threshold limits, while simultaneously reducing the implementation complexity (i.e., the LUT size) by 93%; (ii) achieves comparable transmission performance compared to the MSS-LUT-based DPD, while reducing the implementation complexity by 89%; and (iii) shows great potential for high-speed, low-complexity and memory-efficient intensity modulation and direct detection (IM/DD) UOWC and short-reach optical interconnects.

1. Introduction

Due to the considerable demand for information exchange, there has been a surge of interest in the research of ocean exploration systems in recent years. The limited bandwidth of radio frequency (RF) and acoustic based underwater communication methods has prompted the emergence of underwater optical wireless communication (UOWC) as an appealing and feasible alternative to fulfill the growing need for high-speed underwater data transmission [1]. Notably, seawater displays low attenuation within the 450 to 550 nm wavelength range [2], thus enabling the effective use of visible green and blue lights in UOWC systems. Recently, research of UWOC systems among 1.7 m to 100 m are being proposed successively [3–5]; various commercial UWOC systems including Ambalux UWOC system [6], BlueComm UWOC system [7], etc., have also appeared on market, delivering underwater data transmission at a distance of 40-200 meters.

#516562 https://doi.org/10.1364/OE.516562
Journal © 2024 Received 21 Dec 2023; revised 28 Jan 2024; accepted 5 Feb 2024; published 21 Feb 2024

Optics EXPRESS

Laser diodes (LDs) have long been extensively utilized in UOWC, mainly owing to their remarkable modulation bandwidth and high power density [8]-[9]. The utilization of intensity modulation and direct detection (IM/DD) four-level pulse amplitude modulation (4-PAM) scheme has emerged as an attractive option for use in UOWC due to the advantages of simple architecture, low power consumption, secure links and low installation and operational costs [10–12]. However, the presence of bandwidth-limited transceivers and chromatic dispersion in seawater [13]-[14] may lead to inter-symbol interference (ISI), consequently degrading the transmission performance of high-speed UOWC systems [15]-[16].

Similarly, these aforementioned issues are also observed in IM-DD optical interconnect in data centers (DCs). To mitigate ISI and, therefore, enhance the performance of IM-DD links, several digital pre-distortion (DPD) solutions such as Volterra nonlinear equalizers [17]-[18] and neural network equalizers [19]-[20] have been recently proposed. Nonetheless, the implementation of these solutions introduces significant computational complexity.

To address the challenge of reducing computational complexity and enhancing operational ease and flexibility, researchers have proposed LUT-based DPD schemes [21–26]. However, a key issue with these schemes is the exponential growth of the size of LUT in relation to the memory length. In efforts to strike a balance between the storage memory and the performance of the LUT-based DPD, various approaches, such as the modified LUT-based DPD, delta-sigma modulation assisted LUT-based DPD and multi-symbol simplified LUT (MSS-LUT)-based DPD have been introduced to minimize the required storage memory compared with the full-size LUT [22–26]. Yet, current methods heavily rely on pattern pruning from a single memory-length LUT (e.g., LUT with a memory length of n (LUT-n)), constraining their capability to effectively adjusting both DPD performance and storage memory for different LUTs with varying memory lengths.

In this paper, an adaptive-memory-length LUT (AML-LUT)-based DPD is proposed to further reduce the size of LUT for 4-PAM UWOC. Owing to utilization of adaptive memory length for each pattern in the AML-LUT based DPD, the size of AML-LUT can be significantly reduced without sacrificing performance compared to both the full-size LUT and the MSS-LUT based DPDs. We carry out performance evaluation of the proposed AML-LUT based DPD scheme by transmitting 625 Mbit/s 4-PAM over a 1-m long water tank and compare the results with other DPD schemes. We show that the proposed AML-LUT based DPD (*i*) incurs a marginal power penalty of 0.5 dB at both the 7% hard-decision forward error correction (HD-FEC) and KP4-FEC threshold limits compared with the full-size LUT-7 DPD, while simultaneously reducing the implementation complexity (i.e., LUT size) by 93%; and (*ii*) achieves comparable performance compared to the MSS-LUT based DPD, while reducing the implementation complexity by 89%.

The structure of the paper is organized as follows. In section 1, we introduce the research background, whereas in section 2, we present the technological process of proposed AML-LUT based DPD. In section 3, we discuss the experimental setup and results. Finally, this paper is concluded in section 4.

2. Principle of the proposed AML-LUT-based DPD

2.1. Full-size LUT-based DPD

The full-size LUT-based DPD uses a table to store the pattern information in order to reduce the impact of ISI. In 4-PAM-4 transmission systems, a full-size LUT with a memory length of q (LUT- q) contains 4^q patterns, where each pattern stores its corresponding pattern sequence s and the pre-distortion value e. Table 1 shows the order of the pattern for LUT-3 with an array data structure.

Figure 1 illustrates the flow chart of establishing the full-size LUT in 4-PAM. First, both e_total and N in Fig. 1 are initialized to zero. This is followed by sending a random training sequence from the transmitter (Tx) to the receiver (Rx). The symbol sequence within the sliding

Optics EXPRESS

Table 1. Order of the pattern in LUT-3 for 4-PAM

Index *i*	Pattern Sequence *s*			Pre-distortion Value *e*
1	-3	-3	-3	$e[1]$
2	-3	-3	-1	$e[2]$
.	.	.	.	.
63	3	3	1	$e[63]$
64	3	3	3	$e[64]$

window $x[n\text{-}M]$: $x[n+M]$ contains the specific pattern derived from transmitted 4-PAM symbols $x[n]$ with a memory length of $2M+1$. The instantaneous pre-distortion value for $x[n]$ of a sliding window is given as:

$$\varepsilon[n] = y[n] - x[n], \tag{1}$$

where $y[n]$ represents the corresponding received signal of $x[n]$. With the sliding window moving forward, the sum of pre-distortion value and the count of pattern occurrences for LUT index i are recorded as:

$$e\_\text{total}[i] = e\_\text{total}[i] + \varepsilon[n], \tag{2}$$

$$N[i] = N[i] + 1. \tag{3}$$

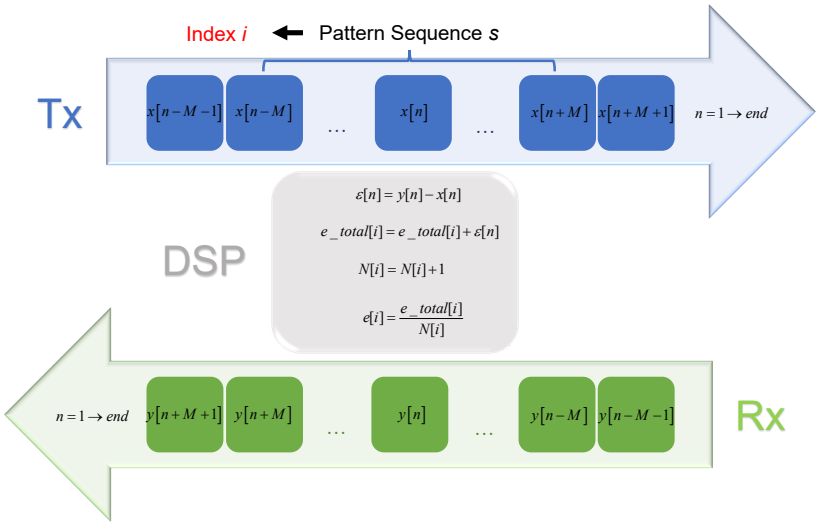

Fig. 1. The flow chart for establishing the LUT in 4-PAM.

After sweeping over the entire training sequence, the averaged pre-distortion value can be calculated by:

$$e[i] = \frac{e\_\text{total}[i]}{N[i]}. \tag{4}$$

Next, $e[i]$ is stored in the LUT while other parameters are removed.

Having created the LUT, the output of the full-size LUT-based DPD is given by:

$$x'[n] = x[n] - e[i]. \tag{5}$$

Optics EXPRESS

2.2. MSS-LUT-based DPD

To reduce the size of LUT, an MSS-LUT based DPD has been proposed to prune some of the patterns [19]. From the histogram of pre-distortion value of a full-size LUT-5 in 4-PAM UOWC depicted in Fig. 2 it can be observed that most distributions are centered around zero, therefore, compensation of patterns close to zero will have negligible impact on the performance of DPD.

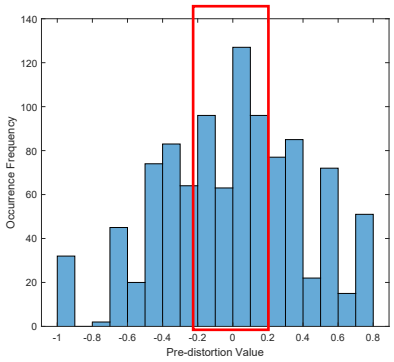

Fig. 2. Histogram of pre-distortion value of a full-size LUT-5 in 4-PAM UOWC.

Based on the aforementioned inference, the MSS-LUT based DPD can be constructed by setting a table-size threshold, which is expressed as:

$$\varphi[\alpha] = \mathrm{A}[\alpha \times \mathrm{MaxIndex}], \tag{6}$$

where A = sort($|e|$,′ ascend′) denotes sorting the sequence e in ascending order, MaxIndex is the maximum index of the LUT and α is a parameter in the range of 0 to 100%. If $e[i] < \varphi(\alpha)$, the corresponding pattern of the LUT can be pruned, thereby reducing the implementation complexity. Note that the resulting size of LUT is proportional to 1-α, which is given by (1-α)×MaxIndex (rounding up if the result is a decimal), thus indicating the implementation complexity of MSS-LUT based DPD.

2.3. AML-LUT-based DPD

The AML-LUT based DPD combines various memory-length LUTs to establish a memory-length-controllable LUT. Different from the full-size LUT as shown in Table 1, this approach incorporates an additional bit error rate (BER) entry to determine the optimal memory length for each pattern. Note that compared with traditional LUT schemes which use the error amplitude as the indictor, BER is used here because the error amplitude cannot reflect the predistortion performance accurately when the memory length is not enough. The error amplitude used in a traditional LUT is the mean error calculated via a large number of samples of one particular pattern and it could have large standard deviations when a short LUT is used, which may lead to high BER in a pattern. For LUT-n, in a similar manner to the full-size LUT a BER table is generated by recording the BER of each pattern following pre-distortion by the full-size LUT-n based DPD. The BER s_BER[i]for the pattern with an index of i is given by:

$$\mathrm{s\_BER}[i] = \frac{err\_n[i]}{N'[i]}, \tag{7}$$

where $err\_n[i]$ and $N'[i]$ represent the number of error pattern and the total number of patterns, respectively. The BER of each pattern is tested by 10 times and the averaged value is calculated in the BER table. Note, for low BERs the LUT requires short memory-length patterns, since

Optics EXPRESS

long memory-length patterns contribute very little to lowering the overall system BER, therefore can be ignored to reduce the storage memory. Conversely, higher BER patterns necessitate the use of long memory-length patterns to achieve the improved performance of DPD.

To quantify the required memory length of each pattern a threshold is set, which is given by:

$$\gamma(\beta) = \beta \cdot \max(\text{s\_BER}), \tag{8}$$

where β is a parameter within the range of 0 to 100% and max(s_BER) is the maximum BER pattern. When s_BER > $\gamma(\beta)$ the pattern is removed from the LUT and is replaced with larger memory-length LUT patterns with for 4-PAM in our experiment. Due to the additional 2 bits are added at the beginning and the end of larger memory length patterns, respectively, for 4-PAM signals, $4 \times 4 = 16$ new patterns is needed to replace the old pattern, as shown in the highlighted block in Table 2.

Table 2. Order of the pattern in an AML-LUT for 4-PAM

Index *i*	Memory Length	Pattern Sequence *s*					Pre-distortion Value *e*
1	3		-3	-3	-3		*e*[1]
2	3		-3	-3	-1		*e*[2]
3	3		-3	-3	1		*e*[3]
4	5	-3	-3	-3	3	-3	*e*[4]
5	5	-3	-3	-3	3	-1	*e*[5]
6	5	-3	-3	-3	3	1	*e*[6]
7	5	-3	-3	-3	3	3	*e*[7]
8	5	-1	-3	-3	3	-3	*e*[8]
9	5	-1	-3	-3	3	-1	*e*[9]
10	5	-1	-3	-3	3	1	*e*[10]
11	5	-1	-3	-3	3	3	*e*[11]
12	5	1	-3	-3	3	-3	*e*[12]
13	5	1	-3	-3	3	-1	*e*[13]
14	5	1	-3	-3	3	1	*e*[14]
15	5	1	-3	-3	3	3	*e*[15]
16	5	3	-3	-3	3	-3	*e*[16]
17	5	3	-3	-3	3	-1	*e*[17]
18	5	3	-3	-3	3	1	*e*[18]
19	5	3	-3	-3	3	3	*e*[19]
.	.	.	.	.	.	.	.
Imax-1	3		3	3	1		*e*[63]
Imax	3		3	3	3		*e*[64]

The implementation complexity can be further reduced by conducting table pattern pruning in AML-LUT. Based on the aforementioned MSS-LUT, patterns with pre-distortion values around zero can be pruned. Before the AML-LUT is established, The MSS-LUT of different memory lengths is tested and the appropriate parameter value $\alpha(n)$ can be ensured, where n is the memory length. Then just like in the MSS-LUT procedure, if the pre-distortion value of an n memory-length pattern sequence $e[i] < \varphi(\alpha(n))$, the corresponding pattern of the LUT can be pruned. Once the final AML-LUT is established, the AML-LUT based DPD operates according to the flow chart shown in Fig. 3. It should be noted that the resulting LUT size of AML-LUT is not proportional to $\gamma(\beta)$, β, or any other parameters. Therefore, the LUT size is chosen to evaluate the implementation complexity of AML-LUT based DPD.

Optics EXPRESS

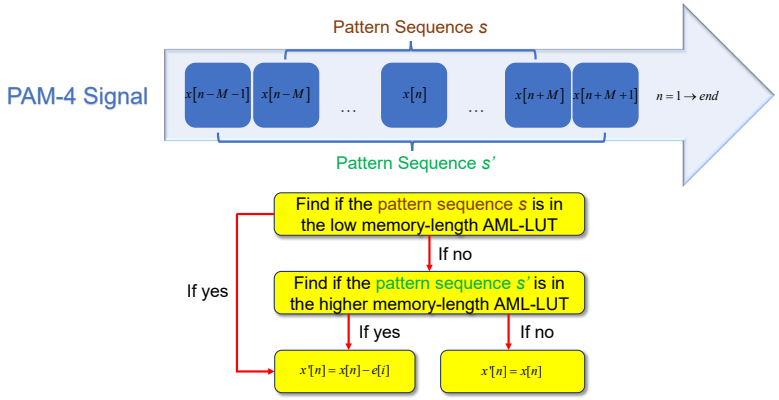

Fig. 3. Flow chart of AML-LUT-based DPD.

3. Experimental setup, simulation and results

3.1. Experimental setup

The performance of the proposed AML-LUT based DPD is evaluated for a 625 Mbit/s 4-PAM UOWC link as shown in Fig. 4. At the Tx, randomly generated 312.5 MBaud Gray-coded 4-PAM symbols are processed by DPD at one sample per symbol. The pre-distorted 4-PAM symbols are then up-sampled to two samples per symbol and pulse-shaped by a root-raised cosine filter (RRC) with a roll-off factor of 0.1. Subsequently, 625 MSa/s 4-PAM is applied to an arbitrary waveform generator (AWG, Tektronix AWG7122C) the output of which is fed into an amplifier (Mini-Circuits ZHL-32A-S) and an attenuator (ATT) prior to intensity modulation of a 450n nm laser diode (LD, Sharp GH04580A2 G) via a bias-tee. In our experiment, we set the LD drive current to 46 mA, which is within the linear regions of both power-current (P-I) and voltage-current (V-I) curves as illustrated in Fig. 5. The modulated light bean is launched into a 1 m long pure water tank, where an agitator is employed to replicate the natural turbulence. Due to

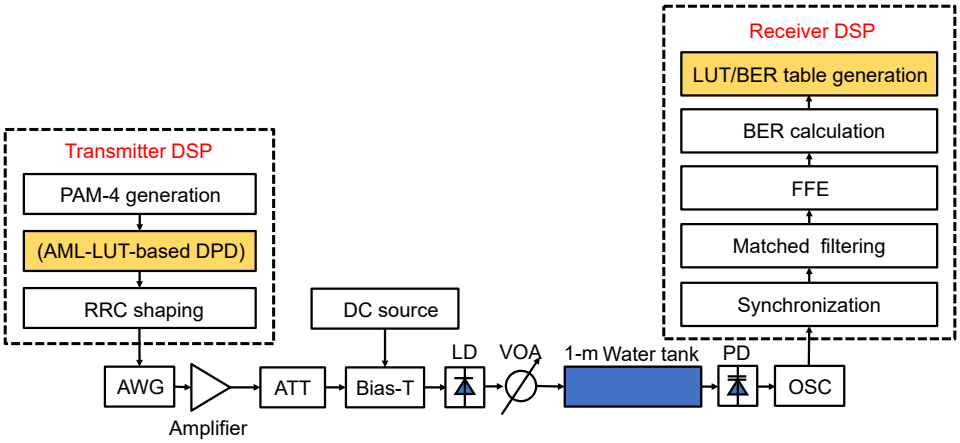

Fig. 4. Experimental setup and DSP block diagram. AWG: arbitrary waveform generator; RRC: root-raised cosine filter; DC: direct current; Bias-T: bias-tee; LD: laser diode; VOA: variable optical attenuator; PD: photo detector; OSC: real-time oscilloscope; FFE: feed-forward equalizer

Optics EXPRESS

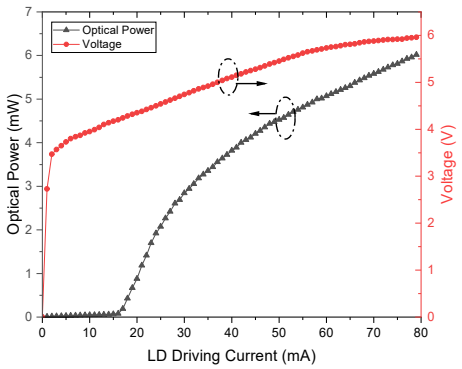

Fig. 5. The output optical power and the forward voltage as a function of the LD drive current working at 25 °C.

the non-vertical incident angle, the PD does not receive reflections from the multi-layer glass. At the Rx, the optical signal is applied to a high-speed Si avalanche photodetector-based Rx (Hamamatsu C12702), the output of which is captured by a digital oscilloscope (OSC, Tektronix DPO73304D) for offline processing. The ISI problem comes from the nonlinearities of the AWG, driver amplifier and the LD, the bandwidth limitations of the LD and PD, and the underwater channel. The off-line processing includes timing synchronization, matched filtering, equalization with a feed-forward equalizer (FFE), BER estimation and LUT/BER table generation.

3.2. Results and discussion

The parameters used in the UWOC system are shown above in Table 3. We firstly optimized the drive voltage of 4-PAM using FFE with a memory length of 201 by adjusting the AWG-output amplitude at a received optical power (ROP) of -6.2 dBm. Figure 6(a) shows the measured signal-to-noise ratio (SNR) as a function of the AWG-output amplitude. As shown, the SNR linearly increases with the AWG-output amplitude reaching the peak value of ~ 16.7 dB at 0.9 V (i.e., the optimum value) beyond which it the SNR reduces due to the nonlinear effects. Figure 6(b) depicts the measured BER as a function of training symbols in MSS-LUT based DPD and AML-LUT based DPD at the ROP of -7.1 dBm. Accordingly, 524288 4-PAM training symbols is chosen in the experiment with 10-time averaging at each run.

Table 3. Parameters of UWOC system

Parameter	Value
ROP (without attenuator)	-6.2 dBm
AWG-output amplitude	0.9 V
memory length of FFE	91
bitrate	625Mbit/s

Next, Fig. 7(a) depicts the measured BER as a function of the memory length of FFE, where lower BER is achieved for longer memory length of 90, beyond which it reaches the saturation level. In this work, to balance the performance and complexity, a memory length of 91 was selected for the subsequent experiment. Next, we evaluated and compared the performance and complexity of different LUT-based DPD schemes. Figure 7(b) shows the measured BER versus the threshold parameter α for the MSS-LUT based DPD at a ROP of -6.2 dBm. It can be seen that utilization of full-size LUT (i.e., MSS-LUT with α of 0) and MSS-LUT based DPD demonstrates a significant reduction in the BER compared to the case without PDP (i.e., MSS-LUT with α of

Optics EXPRESS

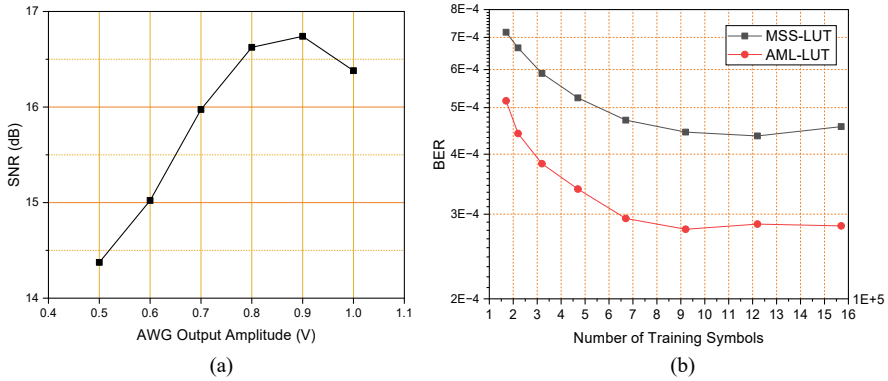

Fig. 6. Measured: (a) SNR as a function of AWG-output amplitude, and (b) BER versus training symbols in MSS-LUT- and AML-LUT-based DPD at the ROP of -7.1 dBm.

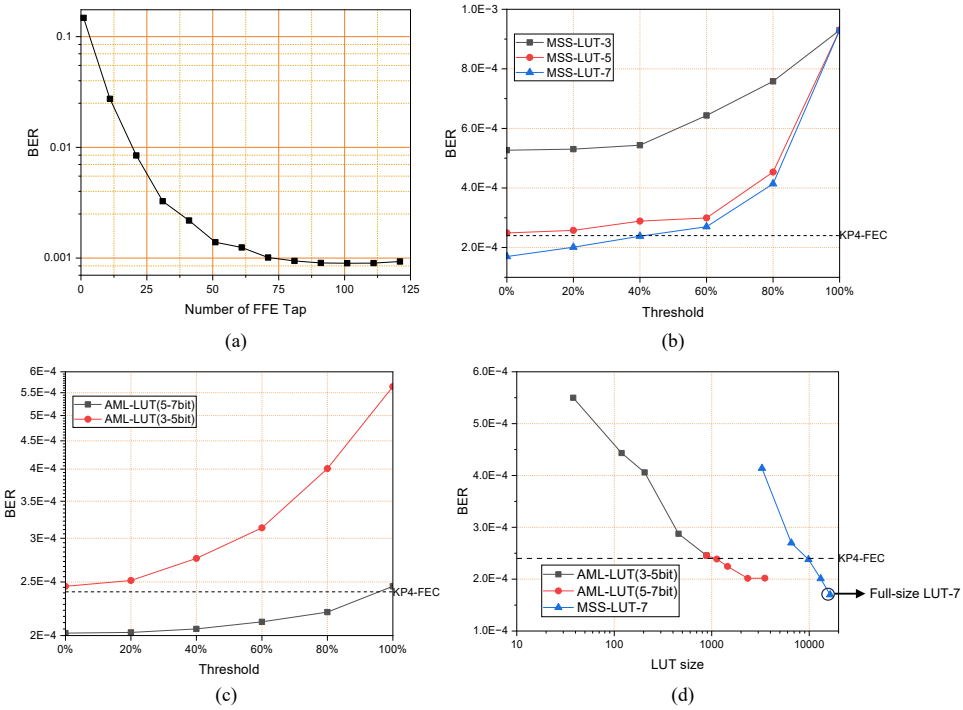

Fig. 7. Measured BER versus the: (a) BER versus memory length of FFE in a 1-m UOWC system at a ROP of -6.2 dBm, (b) threshold parameter α of MSS-LUT-based DPD, (c) threshold parameter β of AML-LUT-based DPD and (d) LUT size for AML-LUT- and MSS-LUT-7-based DPDs.

100%). Furthermore, it is also observed that increasing the memory length of the LUT leads to improved performance of DPD. Note that a memory length of 7 is adequate for supporting 625 Mbit/s 4-PAM transmission with the achieved BER below the KP4-FEC threshold level of 2.4×10^{-4}. The MSS-LUT offers substantial storage size savings when compared to the full-size LUT based DPD, while maintaining satisfactory performance below the KP4-FEC threshold level provided α remains within 40%. Also compared is the implementation complexity of different DPD schemes based on the LUT size. To ensure optimal performance of the proposed

Optics EXPRESS

AML-LUT based DPD, pruning parameters for LUT-3, LUT-5, and LUT-7 in AML-LUT were all set to 20%. Figure 7(c) shows the measured BER versus the threshold parameter β for the AML-LUT based DPD for both 3-5 bit and 5-7 bit at a ROP of -6.2 dBm. As the parameter β arising from 0 to 100%, the slope of BER curve goes up. It should be noted that the BER performance of AML-LUT based DPD for 3-5bit is between the BER performance of LUT-3 and LUT-5 and the BER performance of AML-LUT based DPD for 5-7bit is between the BER performance of LUT-5 and LUT-7.

Figure 7(d) shows BER as a function of LUT sizes for AML-LUT and MSS-LUT-7 based DPDs, the LUT size was calculated by changing parameter α in MSS-LUT and β in AML-LUT. Note, the results do not include MSS-LUT-3 and MSS-LUT-5 cases due to their higher BERs, which are above the KP4-FEC threshold level. The size of AML-LUT is expanded by incorporating various combinations of memory lengths, including 3 and 5 as well as 5 and 7, while the intersection point of these two combinations represents the utilization of a memory length of 5 in AML-LUT. At the selected point, the LUT size of full-size LUT-7 is $4^7 = 16384$, the LUT size of the threshold at KP4-FEC of MSS-LUT-7 is 9830 and the LUT size of threshold at KP4-FEC of MSS-LUT-7 is 1127. By switching form full-size LUT-7 based DPD to the proposed AML-LUT based DPD, the LUT size has 93.1% reduction in implementation complexity; by switching form MSS-LUT-7 based DPD to the proposed AML-LUT based DPD, the LUT size has 88.5% reduction in implementation complexity. All the BER performance of DPDs are below the KP4-FEC threshold level of 2.4×10^{-4} at the selected point.

Finally, the measured BER versus ROP for a 1-m long UOWC link with different DPD together with the corresponding histograms are presented in Fig. 8. To strike a balance between performance and implementation complexity, α is set to 40% for MSS-LUT-7 based DPD while the threshold of proposed AML-LUT based DPD is determined for the LUT size of 1127 for AML-LUT. Note that a significant reduction in BER is achieved for LUT-based DPD schemes with a memory length of 7 compared with the case without DPD. In comparison to full-size LUT-7 based DPD, the proposed AML-LUT based DPD incurs a marginal power penalty of 0.5 dB at both the 7% HD-FEC and KP4-FEC threshold levels, while simultaneously reducing implementation complexity by 93.1% (i.e., corresponding to 15,257 LUT size reduction). Meanwhile, the proposed AML-LUT based DPD achieves comparable BER performance as MSS-LUT based DPD and reduced implementation complexity by 88.5% (i.e., corresponding to 8,703 LUT size reduction). Figure 8(b)–8(e) illustrates the received sequence diagrams of 4-PAM for different LUT based DPDs at a ROP of -6.2 dBm. The experimental results demonstrate the great potential of the proposed AML-LUT based DPD in achieving high-speed, low-complexity

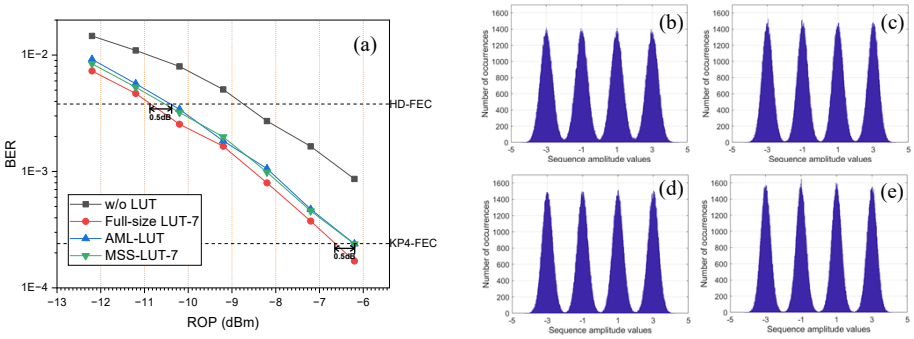

Fig. 8. (a) Measured BER versus ROP using different DPD schemes in a 1-m UWOC system. Received histograms for 4-PAM: (b) without LUT, (c) with MSS-LUT, (d) with AML-LUT, (e) and with full-size LUT-based DPDs at a ROP of -6.2 dBm.

Optics EXPRESS

and memory-efficient IM/DD transmission in both UOWC and short-reach optical interconnect applications.

4. Conclusion

In this paper, we proposed and experimentally demonstrated an AML-LUT based DPD technique for a 4-PAM UOWC system. By employing adaptive memory length for each pattern in the AML-LUT based DPD, we achieved reduced significantly reduced implementation complexity and comparable BER performance compared with full-size LUT and the multi-symbol MSS-LUT based DPDs. Experimental results showed that the proposed AML-LUT based DPD incurs a marginal power penalty of 0.5 dB at the 7% HD-FEC and KP4-FEC threshold levels with reduced implementation complexity (i.e., LUT size) by 93.1% compared to the full-size LUT-7 based DPD. Furthermore, the proposed AML-LUT based DPD achieved comparable transmission performance to the MSS-LUT based DPD with the reduced implementation complexity of 88.5%.

Funding. Science and Technology Planning Project of Guangdong Province (2019A050510039); Basic and Applied Basic Research Foundation of Guangdong Province (2021B1515120057, 2022A1515011258); General Research Fund (GRF) of The Research Grants Council (RGC) of Hong Kong (15231322); Guangdong Provincial Key Laboratory of Optical Information Materials and Technology (2023B1212060065).

Disclosures. The authors declare no conflicts of interest.

Data availability. Data underlying the results presented in this paper are not publicly available at this time but may be obtained from the authors upon reasonable request.

References

1. Z. Zhaoquan, Shu Fu, Huihui Zhang, *et al.*, "A survey of underwater optical wireless communications," IEEE Commun. Surv. Tutorials **19**(1), 204–238 (2017).
2. S. Q. Duntley, "Light in the sea," J. Opt. Soc. Am. **53**(2), 214–233 (1963).
3. F. Huang Y, T. Tsai C, and C. Chi Y, "Filtered multicarrier OFDM encoding on blue laser diode for 14.8-Gbps seawater transmission," J. Lightwave Technol. **36**(9), 1739–1745 (2018).
4. X. Hong, Chao Fei, Guowu Zhang, *et al.*, "Discrete multitone transmission for underwater optical wireless communication system using probabilistic constellation shaping to approach channel capacity limit," Opt. Lett. **44**(3), 558–561 (2019).
5. J. Wang, Chunhui Lu, Shangbin Li, *et al.*, "100 m/500 Mbps underwater optical wireless communication using an NRZ-OOK modulated 520 nm laser diode," Opt. Express **27**(9), 12171–12181 (2019).
6. Stephen Fasham and Shaun Dunn, "Developments in subsea wireless communications," *Underwater Technology* (IEEE, 2015).
7. Mohammad-Ali Khalighi, Chadi Gabriel, Tasnim Hamza, *et al.*, "Underwater wireless optical communication; recent advances and remaining challenges.," *16th international conference on transparent optical networks* (IEEE, 2014).
8. J. Baghdady, Chadi Gabriel, Tasnim Hamza, *et al.*, "Multi-gigabit/s underwater optical communication link using orbital angular momentum multiplexing," Opt. Express **24**(9), 9794–9805 (2016).
9. A. Al-Halafi, Hassan Makine Oubei, Boon S. Ooi, *et al.*, "Real-time video transmission over different underwater wireless optical channels using a directly modulated 520 nm laser diode," J. Opt. Commun. Netw. **9**(10), 826–832 (2017).
10. K. Nakamura, I. Mizukoshi, and M. Hanawa, "Optical wireless transmission of 405 nm, 1.45 Gbit/s optical IM/DD-OFDM signals through a 4.8 m underwater channel," Opt. Express **23**(2), 1558–1566 (2015).
11. Y. Pan, Lianshan Yan, Anlin Yi, *et al.*, "Simultaneous demultiplexing of 2× PDM-PAM4 signals using simplified receiver," Opt. Express **27**(3), 1869–1876 (2019).
12. G.-W. Lu, Ruben S. Luís, Hiroyuki Toda, *et al.*, "Flexible generation of 28 Gbps PAM4 60 GHz/80 GHz radio over fiber signal by injection locking of direct multilevel modulated laser to spacing-tunable two-tone light," Opt. Express **26**(16), 20603–20613 (2018).
13. N. E. Miroshnikova, G. S. Petruchin, and P. A. Titovec, "Estimation of the effect of dispersion on the communication range in a wireless underwater optical channel.," *Systems of Signal Synchronization, Generating and Processing in Telecommunications* (IEEE, 2021).
14. C. Ju, Na Liu, Xue Chen, *et al.*, "SSBI mitigation in A-RF-tone-based VSSB-OFDM system with a frequency-domain Volterra series equalizer," J. Lightwave Technol. **33**(23), 4997–5006 (2015).
15. W.-S. Tsai, Chung-Yi Li, Hai-Han Lu, *et al.*, "256 Gb/s four-channel SDM-based PAM4 FSO-UWOC convergent system," IEEE Photonics J. **11**(2), 1–8 (2019).
16. C. Shen, Yujian Guo, Hassan M. Oubei, *et al.*, "20-meter underwater wireless optical communication link with 1.5 Gbps data rate," Opt. Express **24**(22), 25502–25509 (2016).

Optics EXPRESS

17. Y. Zhou, Junwei Zhang, Chao Lu, *et al.*, "Low-complexity frequency-domain nonlinear equalizer with absolute operation for underwater wireless optical communications," Opt. Express **31**(14), 23086–23094 (2023).
18. Y. Dai, Xiao Chen, Xingqi Yang, *et al.*, "200-m/500-Mbps underwater wireless optical communication system utilizing a sparse nonlinear equalizer with a variable step size generalized orthogonal matching pursuit," Opt. Express **29**(20), 32228–32243 (2021).
19. Chu Yunhui, Fan Chen, John Lang, *et al.*, "Equalization with neural network circuitry for high-speed signal link.," *International Symposium on Electromagnetic Compatibility, Signal & Power Integrity* (IEEE, 2019).
20. Q. Zhou, F. Zhang, and C. Yang, "AdaNN: Adaptive neural network-based equalizer via online semi-supervised learning," J. Lightwave Technol. **38**(16), 4315–4324 (2020).
21. P. Gou, Li Zhao, Kaihui Wang, *et al.*, "Nonlinear look-up table predistortion and chromatic dispersion precompensation for IM/DD PAM-4 transmission," IEEE Photonics J. **9**(5), 1–7 (2017).
22. J. Zhang, Pengqi Gou, Miao Kong, *et al.*, "PAM-8 IM/DD transmission based on modified lookup table nonlinear predistortion," IEEE Photonics J. **10**(6), 1–9 (2018).
23. He Zonglong, Jinxiang Song, Christian Häger, *et al.*, "Symbol-based supervised learning predistortion for compensating transmitter nonlinearity.," *European Conference on Optical Communication* (IEEE, 2021).
24. Z. He, Jinxiang Song, Kovendhan Vijayan, *et al.*, "Periodicity-enabled size reduction of symbol based predistortion for high-order QAM," J. Lightwave Technol. **40**(18), 6168–6178 (2022).
25. Y. Tu, Xiang Meng, Cheng Wenzhuo, *et al.*, "Simplified Look-Up Table (LUT) Based Digital Pre-Distortion for 100 GBaud/λ PAM-4 Transmission," J. Lightwave Technol. **42**(1), 158–165 (2024).
26. X. Zeng, M. Fu, L. Yi, *et al.*, "Digital Pre-distortion Based on Delta Sigma Modulation Assisted Look-up Table for Optical Transmission," *European Conference on Optical Communication* (IEEE, 2022).